NORDIC VOLCANOLOGICAL INSTITUTE 8803

THE KRAFLA AIR-FALL, WELDED TUFF LAYER, NORTH ICELAND

by

GINA MARIE CALDERONE

REYKJAVIK

MAY 1988

NORDIC VOLCANOLOGICAL INSTITUTE 8803

THE KRAFLA AIR-FALL, WELDED TUFF LAYER, NORTH ICELAND

by

GINA MARIE CALDERONE

REYKJAVIK

MAY 1988

This is a preliminary report from the Nordic Volcanological Institute and should not be referenced or otherwise disclosed without the written permission of the author.

NORDIC VOLCANOLOGICAL INSTITUTE 8803

THE KRAFLA AIR-FALL WELDED, TUFF LAYER, NORTH ICELAND: ANALYSIS OF THE PRODUCTS OF MIXING ACIDIC AND BASIC MAGMA

by

Gina Maria Calderone

Internal Report, Nordic Volcanological Institute, University of Iceland, 101 Reykjavik, May 1988

ABSTRACT

A welded tuff layer at Krafla in northern Iceland, is comprised of five air-fall units which form a ring along the margins of the Krafla caldera and has been associated with a caldera collapsing event occuring during the last interglacier period. The units include: silicic acidic ash, basaltic scoria, intermediate vitrophyre, intermediate spatter, and intermediate rheomorphic tephra deposits. The eruption occurred during the last interglacial period in Iceland, 70,000 to 100,000 years ago, approximately the age of the Krafla caldera. The eruption products indicate that the eruption began with an explosive Plinian ash phase which later changed to Strombolian, spatter forming, activity. The final phase of the eruption has the appearance of Hawaiian style volcanism. The products are extremely welded and exhibit subsequent downslope flow structures. The layer

is thickest (50 meters) along the caldera margins and thins to the north and in an east-west direction. Isopleth maps indicate a general source area for the eruption to be in the southeastern part of the present caldera. The volume of exposed eruption products is 0.3 km3. The estimated original volume for the layer, assuming it to have originally covered the caldera floor, would be 1.4 km3. This volume would account for a 26-30 m subsidence of the 47-50 km2 caldera. Drill hole data along the southern margins of the caldera reveals the presence of the layer at a depth of 290 m below the caldera floor, which indicates displacement of the layer to be greater than 200 m at this location. The chemical variation of whole rock and plagioclase indicates that the layer is a mixture of basic, silicic and intermediate compositions, where the basic component is minor. Silica content in whole rock analysis range from 69-50% and plagioclase compositions range from An20 to An90. Petrological characteristics such as mafic clotting with high An plagioclase and compositionally separate zones in the matrix suggest incomplete mixing of silicic and basic magmas. The layer was formed by an explosive silicic eruption triggered by basaltic magmatism and heterogenous mixture of the two liquids. Rheomorphic features of the layer are explained by different cooling rates of the incompletely mixed magmas.

INTRODUCTION

Tectonic activity in the axial rift zone, in north Iceland (figure 1) is concentrated into five swarms of

faults and fissures each containing a central volcano. The Krafla caldera, measuring 10 km east-west to 7 km north-south, is in the center of the Krafla fissure system. The caldera is thought to have formed during the last interglacial period, 70,000-100,000 years ago (Björnsson, et al., 1977, 1979) and to be related to the explosive eruption which produced the welded Krafla Layer. This layer is the subject of the present report. The caldera is filled by multiple eruptions of younger hyaloclastites and lava flows (Saemundson, 1978, 1979).

Recent explosive, phreatomagmatic events have occurred within the caldera such as the Viti explosion (1724), ejecting mostly silicic pumice, basaltic scoria and hydrothermally altered material. Smaller phreatic and phreatomagmatic eruption craters are dispersed within the caldera. High volumes of intrusive and effusive activity combined with crustal extension at Krafla are acting to widen and conceal the caldera. The most recent of the eruptions are well documented and include: the Myvatn Fires of 1724-1729 (Grönvold, 1984) and the Krafla Lavas since 1975 (Grönvold and Makipaa, 1978)

The Krafla Layer can be separated into five air-fall units of variable distribution, tephra size, welded character and compositional range. These criteria are used to distinguish each of the individual units in the Krafla Layer which is a result of a multiphase eruption of approximately 1.2 km3 of magma.

This paper attempts to assess plausible magmatic and eruptional processes which may have invoked and preceded the welded and heterogeneous nature of the Krafla Layer. The

documenting of the stratigraphic and chemical sequence of the five air-fall units and the analyses of the rocks and plagioclase for each of the units, provide insight into the processes occurring during the interglacial activity of the volcano which have contributed to the welded charactistics and the secondary flow movement of the layer. Volume data presented in this paper indicate the spatial relationships between the layer and the caldera.

STRATIGRAPHY AND DESCRIPTIVE FEATURES

The Layer is a composite of several diverse facies (which will be referred to as units in this report) consisting of generally silicic tephra (69% silica), basic lapilli scoria (50% silica) and intermediate spatter and densely welded spatter and lapilli tephra (59% to 61% silica). The completely transitional stratigraphic relationships between each of the units indicate a relatively short eruptional episode that began with Plinian style activity later evolving into more effusive Strombolian activity within the same eruption.

The Krafla Layer is a hybrid magma composed of a basaltic and a silicic end members. The layer offers insight into two fundamental processes: (1) how composite magmas are erupted; and (2) what physical and chemical conditions are responsible for the welding process.

Hybrid air-fall tuffs, in Iceland, similar to the Krafla Layer, are generally related to silicic explosive eruptions, in some cases with a caldera collapse. In the past, the Krafla Layer has been considered a product of the caldera

collasping event (Saemundsson, 1974, Bjornsson, 1977, 1985).

The Krafla Layer is exposed in thick sections at two localities (figure 2): (1) to the southwest and to the north of Hagong; and (2) near Hlidarfjall mountain. Thinner exposures are found near Gaesafjoll and at Halaskogarfjall. At the Hagong exposures, the layer is the thickest (50 meters) and thins gently to the north. One isolated gully in northern Hagong near Eilifsvotn is relatively thick, up to 10 meters, and appears to be localized accumulation. Most sections on the east flanks of Hagong are about 15 to 20 meters thick. The entire layer follows the irregular basement topography clearly showing its air-fall character; the base dips gently to the southeast and follows the subglacial hyaloclastite formation. The thickness of the western outcrops at Hlidarfjall range from 6 to 10 meters and decrease in thickness to the north. The layer dips gently 10 degrees to the south. To the west, the layer covers subaerial lavas and hyaloclastite formation.

MORPHOLOGY

The degree of welding ranges greatly within the layer; the state of welding within each of the units increases within the layer with straitgraphic height. To describe the degree of welding the following terminology will be used:

1. A "consolidated unit" is held together loosely resulting in a friable consistence. These units consist of ash (<2 mm) and lapilli (2-64 mm) size tephra. These finer size tephra are slightly less consolidated than the larger lapilli (which range 50 mm to 64 mm) and agglomerates (over 64 mm)

size tephra.

2. Spatter bombs (over 20 cm) exhibit various degrees of welding from agglutinated to densely welded. "Agglutinate spatter" are usually ropy, unflattened, and incipiently adhere to adjacent spatter creating void space.

3. "Welded spatter" are defined as the tephra which is adhering to adjacent spatter on all faces, where no void space is maintained. The spatters are found flattened and stretched.

4. A "densely welded" unit characteristically contains lenses of tephra which has become extremely flattened and deformed and where the original tephra size is not always apparent. These units occur in lenses which grade upsection into the top unit of the layer and resemble a typical lava flow.

5. A "fiamme" (Ross and Smith, 1961, p.4) is the flattened and stretched glassy lenses found in the densely welded units.

Unit descriptions

The layer is subdivided into five air-fall units, A, B, C, D and E based on: (1) tephra size distribution and composition, (2) the abundance of pumice and lithic fragments, (3) welded and rheological character; and (4) vertical variation in oxidation state (color). Each of the units are commonly separated by lithic zones (figure 4). The units grade continuously upward with no apparent depositional breaks. They appear to be derived from a

single, continuous eruption event.

Unit A, fine-grained ash: This stratigraphic unit at the base of the stratigraphic sequence ranges in thickness from 20 cm at Hlidarfjall, to 300 cm at the Eilifsvotn section. This is a well-sorted ash, with small (<5 mm) lithics and pumice lapilli. This unit is found in only two localities: Hlidarfjall and Hagong. At Hlidarfjall, unit A is fine-grained, compacted and grades into a reversely graded, lithic zone (40 cm). At the north Hagong locality (near lake Eilifsvotn) the tephra is of coarser grained and contains greater amounts of pumice. It grades upward into the black, lapilli scoria of unit B. This unit occurs at elevations of about 520 m.

Unit B, black lapilli scoria: A black vesicular, consolidated, lithic rich scoria. Lithics range in size from 5 to 20 cm and make up approximately 3% of the unit. The lithics are commonly granophyric and gabbroic in texture. These lithics were most likely incorporated into the magma during ascent and are therefore referred to as xenoliths. This layer occurs at an elevations of about 525 m with an average thickness of 1 m.

Unit C, vitrophyre: The third stratigraphic unit (C) is a black vitrophyre unit, which ranges in thickness from 20 cm to 1 m. Lithics (less than 14 cm) are sparsely distributed throughout the unit, include gabbro, basalt and other volcaniclastic fragments. The unit has a gradational contact with the underlying (B) and the overlying (D) unit. Along both contacts, the vitrophyre disassociates into scoriaceous

pods which grade into the overlying and underlying facies. These pods eventually may become flattened and glassy lenses upsection (figure 5). This unit occurs at elevations of about 530 m.

Unit D, welded spatter: This unit forms the bulk of the entire Krafla Layer and is red due to iron oxidation (table 1). It consists of agglutinated and welded spatter bombs. The spatter ranges in size from 20 cm to 1 m in length and generally increases in size upsection. Agglutinated spatter is concentrated at the base of the unit. Flow structure features become apparent towards the upper portion of D. Lithic blocks are largest (up to 2 m) at the base of the welded spatter unit, above unit C. The measurements of lithic fragments from unit D were used to construct an isopleth map (figure 6). Unit D contains an average of 3% lithics and about 4% in the less welded zones. Large (up to 60 cm) cored bombs are also scattered throughout the unit. Unit D occurs at elevations of about 540 m and has an average thickness of 7 m and a maximum thickness of 25 m (southeast Hagong).

Unit E, densely welded tuff: The top layer (E) is found an the top of Hagong at an elevation of 600 m. It has an average thickness of 5 m and an maximum of 8 m. This unit contains lava-like flow structures and a high percent of lithic fragments. At the base, the unit is occasionally is made up of spatter and lapilli size tephra without welding The layer drapes the topography and thickens along the south and west rims of Hagong. Columnar jointing (plunging up to 10 degrees from the vertical) and spheroidal weathering

features are common. On the top surface of Hagong, ropy surfaces occur locally. Flow structures concentrated along the flanks of Hagong seem to increase with increasing slope angle.

WELDING AND RHEOLOGICAL CHARACTERISTICS OF THE UNITS

Flow Features

Flow structures which accompany the welded zones of the layer suggest a post-depositional, rheomorphic origin. Downslope mass flow movements seem to have occurred in the upper 8 to 10 meters (unit E) of the layer (figure 7). The welded and rheomorphic characteristics, interpreted below, are found in about 70% of the entire layer and include the following:

(1) Stretched and flattened fiammes. These glassy lenses increase in flattening and distortion upward within the layer. Arithmetical flattening ratios (Peterson, 1979) calculated for the fiammes in unit D, based on twenty measurements per locality, indicate an increase in flattening towards the south-west of Hagong (figure 4, a and b), near the thickest points of the deposit which also coincides with the area of largest lithic sizes.

(2) Stretched and flattened vesicles along the upper portions of unit E, indicate secondary mass flow of the upper 8 to 10 meters of the layer after deposition.

(3) Minute (2 to 3 cm) fluidally arranged flow veins containing small lithic fragments (<5 cm) are commonly

present throughout unit E.

(4) Spindle shape voids are common in the welded spatter unit (D). These void spaces may contain lodged lithic fragments ranging from 10 cm to 40 cm which appear to have been rotated from their original positions. These subtle features may be an indication of differential flow around a lithic inclusion while the matrix is in a fluid state. In some cases the lithic fragments have become dislodged.

(5) The most prominent secondary flow structures (Chapin and Lowell, 1979; Billings, 1972, Wolff and Wright, 1981; Schmincke and Swanson, 1967) of the Krafla Layer are found at the top of unit E which flows over and beyond the welded spatter unit and proceeds to flow down the steep slopes of Hagong.

According to Ross and Smith (1967) distorted and stretch fabrics developed during welding are dependent on the degree of plasticity, which is related to chemical composition, temperature, compressive overload pressure and the rate of cooling. Although rheomorphic textures are most common in peralkaline compositions, as those from the Canaria Islands (Schmincke and Swanson, 1967) and Pantelleria (Wolff and Wright, 1982), these textures may also occur in calcalkaline rhyolitic compositions (Chapin and Lowell, 1979).

Several factors must have contributed to the development of dense welding and rheomorphism in the Krafla Layer. (1) The relatively low percentage (3%)of lithic clasts dispersed throughout units D and E coincides with high degree of welding (also noted at the Bandelier Tuff, Eichelberger and

Kock, 1979). Welding clearly decreases with increasing lithic percentages. Abundant lithic fragments indicate explosive events that preceded epochs of high effusion rates. The inverse relationship between welding and abundance of lithic fragments is, therefore, an effect of eruption mechanism, where explosions precede high rate effusion rate of magma. (2) Since no correlation exists between the thickness of the layer and welding, accumulation rates were likely to have had no great influence on the degree of welding.

The emplacement temperatures must have remained relatively high inhibiting crystallization of the intermediate glass and matrix. The mixing of basaltic and rhyolitic magmas with widely different solidus temperatures seems to have allowed for longevity of higher plasticity in the layer than expected by purely silicic magmas.

INTERPRETATION OF ERUPTIVE PHASES AND RECONSTRUCTION OF THE ERUPTION

The Early Phase

The grain size and dispersal of the Krafla Layer indicates changing eruption mechanism. The lower stratigraphic units (A, B) consist of acidic ash and basaltic lapilli scoria tephra. These tephra are thickest at localities farthest from the supposed vent location.

The reversely graded lithic horizon above unit A, at Hlidarfjall, may represent an increase in eruption energy during the initial stages of the eruption. Such an increase in energy may affect the welding degree of the ash and raise the height of the eruption column enabling larger fragments

to be transported to greater distances from the source (Self, 1976; Booth, 1973). The beginning explosive stage of the eruption is indicative of Plinian type eruption style. (Wright, et al., 1980; Walker, et al., 1984; Walker, 1981; Walker and Croasdale, 1972; Williams, 1983).

The vitrophyre unit (C) is also thought to have been deposited during this phase of high eruptive energies. After the deposition of the vitric unit, the energy of the eruption decreased and a less explosive style prevailed.

The Late Phase

The later eruption products include spatter (> 30 cm), welded spatter and larger lapilli size tephra (> 50 mm) intermediate in composition. These deposits (units D and E) are thickest at the caldera margins and are at maximum thickness at southwest Hagong close to the probable source. The eruption style seems to have changed to fire-fountaining production and Strombolian to Hawaiian activity and is referred to as the Strombolian phase.

Figure 8, in a schematic section of the layer with the proposed eruption mechanisms. It is noted that the most extensive welding is confined to the mixed upper units produced during Strombolian to Hawaiian stages of the eruption.

The waning explosive nature of the entire eruption may also be as an indication of decreasing variability in the magma viscosity and volatile content (Cas and Wright, 1987; McBirney and Murase, 1984; Sparks and Pinkerton, 1978).

THICKNESS AND SOURCE AREA

The Krafla Layer generally decreases in thickness and dips up to 10 degrees away from the present caldera margins. The lithic size (long axis) and large thickness for the Strombolian phase are both at maximum in the south-eastern portion of the present caldera (figures 6 and 9). This area is roughly east of Krafla mountain and is considered a plausible source area for the eruption (figure 2).

The Plinian deposit is thickest in the southwest and northeast, near Hlidarfjall and northeast Hagong. The ash unit (A) is much thinner (30 cm) and of finer grain-size in the southwestern exposure than in the northeastern exposure (3 m) where the ash is mixed with large lapilli tephra (> 30 mm). This difference may be caused by wind directions during the eruption or possibly due to separate vents along a ring fracture.

Modeling plots of spatter size, lithic size and thickness distribution for each of the eruptive phases (figure 10) versus distance from a point area within the caldera (figure 2) were derived from isopeth and isopach maps of the layer and lithic sizes (figures 6 and 9) and indicate the point to be the plausible source for the Strombolian phase. The spatter size distribution (figure 10c) exhibit an irregular curve when plotted against source distance. The larger (60 to 40 cm) median spatter sizes (longest axis) found in sections F, E, D and A are located at Hlidarfjall and Hagong (figure 2). Spatter sizes at section G near Gaesafjall are justifiably relatively small (20 cm) in accordance with a source area was close to southeast Hagong.

VOLUME ESTIMATES FOR EACH OF THE UNITS

The volume of the Krafla Layer was calculated from the thickness and area of each of the five units with the assumption that the layer was deposited within the original Krafla caldera. Recent rifting and the addition of new crust to the area have acted to widened the caldera since interglacial time. The area of the caldera during the deposition of the Krafla Layer, is estimated at 47 km2 by considering the caldera fault maps (Saemundson, 1982) and the rate of spreading in the neovolcanic zone (Björnsson, et al., 1979).

Table 2 shows the maximum volume for the entire Krafla Layer to be at about 1.4 km3. The existing outcrop of the layer is at about 0.3 km3. The dense rock equivalent (DRE) has been calculated by measuring the area of one cubic rock sample for each of the units and using the glass density for the respective silica content. The (DRE) volumes for each of the units indicates the acid phase (unit A and C) is 0.081, the basic phase (unit B) is 0.060 and the intermediate phase (unit D and E) is 1.09 km3. The basic magma was relatively in minor amounts.

It is concluded that the Krafla Layer was formed by an eruption just prior to or during a caldera collapsing event of the central volcano. The total DRE volume of the layer (1.23 km3) only can account for a 26 m to 30 m subsidence of the original 47 km2 caldera. Topographical relationships between the elevations of the layer outcrops and the caldera floor indicate subsidence of at least 150 m. The layer has not been found in drill holes within the center of the

caldera (Gudmundsson, et al., 1983), but has been found in one drill core (figure 2) near Halaskogarfjall, at a depth of 275 to 290m, along the southern original margin of the caldera. The total displacement of the layer at this point is maximumally 300 m. Based on the original caldera size and the drill hole data, the caldera volume can be estimated at 14.1 km3. The volume relationship between the layer and the caldera indicates that (1) this eruption could only account for a minor extent of the caldera displacement and; (2) the volume of the layer is minute in comparison to the total subsidence at Krafla which indicates that subsidence has continued since this eruption attaining up to 300 m below the caldera floor.

STRATIGRAPHIC VARIATIONS IN SELECTED WHOLE ROCK AND PLAGIOCLASE COMPOSITIONS

Whole Rock Analyses

Three compositional groups are found in the Krafla Layer (table 3): an acidic, a basic and an intermediate group. The rocks range from an icelandite to dacite composition for unit A, a tholeiitic icelandite for unit B and units C, D and E range within icelandite compositions (Carmichael, 1984)

The AMF triangular diagram for whole rock analyses (figure 11) indicates the general compositional similarities between the Krafla Layer and younger evolved rocks and basaltic lavas from the Krafla-Namafjall fissure swarm (Grönvold, 1972, 1978, 1984). The comparative diagram indicates the siliceous unit A and the iron-magnesium rich unit B (for example, samples A-1a, A-1, A-3, B-1, B-11,

table 3) plot significantly close in composition to the rhyolitic Namafjall and tholeiitic Krafla Lava flows, respectively.

Variation diagrams of the major elements in the five units indicate linear trends (figure 12). With increasing SiO2 content, K20 and Na20 increase and FeO, MgO, CaO, TiO, P205 decrease. The major element variations in the stratigraphic sections show that the base unit is the most evolved, the second eruptive unit B is the least evolved and is overlain by eruptive units which are silica and alkali enriched to intermediate compositions which comprise the bulk of the layer. The whole rock analyses together with the stratigraphic order the units indicate that the eruption occurred from a chemically heterogeneous source or multiple magma chambers.

Mineral and glass analyses

The major minerals present in the Krafla Layer are plagioclase and minor proportions of quartz, clinopyroxene, titanomagnetite and apatite. Quartz is most abundant in units A; clinopyroxene is associated with high An plagioclase crystals in glomercryst clots common to units B, and the intermediate units (table 4). Magnetite and titanomagnetite occur throughout the layer.

The plagioclase analyses for the tephra units (table 5 and appendix 1) show a wide compositional range. The bulk of the plagioclase compositions are bimodal, ranging from An45-65 to An80-90. A minor population of sodic plagioclase, An20-25, exists in units A and B (figure 13). Microprobe analyses across plagioclase grains indicate that

reverse zoning is not present in any of the units which excludes recent partial melting effects on an originally sodic plagioclase.

Calcium enrichment occurs in the large (2 mm) plagioclase megacrysts in unit B and in the mafic glomerocrysts. Glomerocrysts are comprised of plagioclase laths (0.2 mm) An70-80 and fragments of clinopyroxene crystals, which are lodged more toward the center. The occurrence of the mafic clots in intermediate and evolved tephra types is associated with coeruptive acid-basic magmas and incomplete mixing of the two (Gill, 1980, p. 269; Walker, 1983; Eichelberger and Gooley, 1977; Eichelberger, 1980). Microprobe analyses of the streaky matrix textures in the heterogenous welded unit (D) indicate that these microtextures are compositionally zoned, comprised of acidic and basic counterparts in both plagioclase and glass compositions (table 4 for glass compositions). These compositional zones in the matrix are significant due to their association with incomplete magma mixing processes.

Chemical heterogeneity indicates that the mixing of two end members (A and B) are capable to yield the daughter compositions within the range of units C, D, E, and explains the variation in plagioclase and glass compositions.

SUMMARY AND CONCLUSION

Eruption and Magmatic Process

The stratigraphic positioning, major element and plagioclase variations represent separate eruption phases of compositionally different magmas.

In the early Plinian phase an acid magma erupted just prior to basic magma. The two depositional units erupted during this phase reveal an explosion of a silicic reservoir that was subsequently penetrated by a basaltic magma (B).

During the second phase more time may have been allowed for mixing where a bulk intermediate composition was derived from a mixture of compositions similar to the acid and basic magmas. The heterogenous character of the eruptive units such as welding, streaky matrix compositions, glomerocryst clotting and compositionally separated plagioclase and glass populations indicate that the intermediate hybrid had little time for complete mixing and equilibration in the ascent path to the surface. Volume estimates show that the acid magma existed in minor amounts as compared to the basic portion.

The injection of even a minor amount of basaltic magma into a more evolved magma can lead to superheating of the latter, resulting in an explosive Plinian eruption (Sparks, et al., 1977). The less explosive Strombolian phase, which later prevailed in the eruption, seems to have occurred while the two magmas were only incipiently mixed and still in a compositionally heterogeneous state. The units of the early phase (A and B) also show compositionally mixed glass, variable plagioclase compositions and scattered mafic clots. This suggests that units A and B have possibly undergone some mixing prior to the eruption.

Mixing Magmas and the Welding Process

The second phase of the eruption characteristically

exhibits the highest variability in welding character ranging from agglutinated spatter to the densely welded spatter lenses. These variations in welding also exist solely in the intermediate fall units (D and E) which are compositionally the most hybridized units.

The welding characteristics and various secondary flow structures in the layer are inferred to be related to the effects of mixing acid and basic magmas. A hotter basaltic magma acts to hold the acid magma at higher temperatures long enough to allow for post-depositional plastic flow movement in the deposit. It is therefore concluded that hybridization of magmas was the primary cause of welding in the Krafla Layer.

Conclusions

The units of the Krafla Layer are separated compositionally as well as on the basis of tephra size and welding charactistics.

The size and distribution of the eruption products indicate the eruption to have occurred in separate phases: an initial Plinian phase carrying both acid and basic tephra followed by a Strombolian phase carrying incompletely mixed intermediate tephra with highly different degrees of welding and post-depositional flow structures.

The source area of the layer has been localized by thickness measurements, tephra size and lithic fragment size distributions to be in the southeast part of the present-day caldera.

The magma reservoirs giving rise to the Krafla layer were (1) a basaltic reservoir of a composition similar to the

recent tholeiitic lavas within the caldera; and (2) a less voluminous dacitic reservoir of a composition matching the evolved extrusive rocks are found outside the caldera rim.

As inferred from the stratigraphic sequences of the layer, the silicic initial phase of the eruption was triggered by the injection of basaltic magma into an evolved magma chamber. The opening, explosive phase opened up an easy ascent path for the basic magma which resulted in an exceptionally high rate of effusion. It is suggested that high volume, explosive eruptions, from a shallow source, such as the Krafla Layer and the 1875 eruption in Askja, precede a caldera collapse and since no other process could open the ascent paths capable of maintaining sufficiently high productivity. Accordingly, the presence of a shallow, silicic magma chamber played an important role in the formation of the Krafla caldera. The explosion of the silicic chamber, causing a sudden pressure release, was followed by an eruption of a basaltic magma at a high effusion rate. The magma replenishment from the mantle presumably had not counteracted the resulting volume changes. Accordingly, the eruption rates exceeded the refilling rate of the shallow chamber.

ACKNOWLEDGMENTS

This work was supported by a Fulbright Grant and the Nordic Volcanological Institute. I thank the Nordic Volcanological Institute for facilitating this research.

REFERENCES

Billings, M.P., 1972. Structural Geology, 3rd edition. Prentice-Hall Inc., Englewood Cliffs, New Jersey, pp 373-378.

Bryan, W.B., Finger, L.W. and Chayes, F., 1969. Estimating proportions in petrologic mixing equations of least squares approximation. Science, 163: 926-927.

Björnsson, A., Johnsen, G., Sigurdsson, S., Thorbegsson, G. and Tryggvason, E., 1979. Rifting of the plate boundary in northern Iceland. J. Geophys. Res., 84: 3029-3038.

Björnsson, A., Saemundsson, K., Einarsson, P., Tryggvason, E., and Grönvold, K., 1977. Current rifting episode in north Iceland. Nature, 266: 318-323.

Booth, B., 1973. The Granadilla pumice deposit of southern Tenerife, Canary Islands. Proc. Geol. Assoc. London, 84: 353-370.

Carmichael, I.S.E., 1964. The petrology of Thingmuli, a Tertiary volcano in eastern Iceland. J. Petrol., 5: 435-460.

Cas, R.A.F., and Wright, J.V., 1987. Volcanic Successions: Modern and Ancient. Allen and Unwin Ltd., pp 129-265.

Chapin, C.E., and Lowell, G.R., 1979. Primary and secondary flow structures in ash-flow tuffs of the paleovalley, central Colorado. In: C.E. Chapin and W.E., Elston

(Editors), 1979. Ash-Flow Tuffs. Amer. Geol. Soc. special paper 180: pp 137-154.

Eichelberger, J.C. and Gooley, R., 1977. Evolution of silicic magma chambers and their relationship to basaltic volcanism. Geophs. Monograph, 20: 57-77.

Eichelberger, J.C. and Koch, F.G., 1979. Lithic fragments in the Bandelier Tuff, Jemez Mountains, New Mexico. J. Volcanol. Geotherm. Res., 5: 115-134.

Eichelberger, J.C., 1980. Vesiculation of mafic magma during replenishment of silicic magma reservoirs. Nature, 288: 446-450.

Fisher, R.V. and H.-U. Schmincke, 1984. Pyroclastic Rocks. Springer-Verlag, Berlin, Heidelberger, New York, pp 128-218.

Gill, J.B., 1981. Orogenic Andesites and Plate Tectonics. Springer- Verlag, Berlin, Heidelberger, New York, pp 168-294.

Grönvold, K., 1972. Structural and Petrochemical Studies in the Kerlingarfjoll Region, Central Iceland, Ph.D thesis, Univer. of Oxford, pp 1-237.

Grönvold, K., and Makipaa, H., 1978. Chemical composition of the Krafla Lavas 1975-1977. Nordic Volcanol. Institute, report 7816: 1-28.

Grönvold, K., 1984. Myvatn Fires 1724-1729, chemical composition of the lava. Nordic Volcanol. Institute, report 8401: 1-49.

Gudmundsson, A., Sigursteinsson, D., Gudmudsson, G., Fridleifsson, G.O., Tryggvason, H., 1983. KRAFLA HOLA KJ-22, Orkustofnun report OS 8-070, JHD-2B: 4-6

Irvine, T.N., and Baragar, W.R.A., 1971. A guide to the chemical classification to common volcanic rocks. Canadian J. Earth Science, 8: 523-548.

Jogensen, K., 1980. The Thörsmork Ignimbrite: an unusual comenditic pyroclastic flow in southern Iceland. J. Volcanol. Res., 8: 7-23.

McBirney, A.R. and Murase, T., 1984. Rheological Properties of Magmas. A. Rev. Earth Planet Science, 12: 334-357.

Peterson, D.W., 1979. Significance of flattening of pumice fragments in ash-flow tuffs. Geol. Soc. Amer. special paper 180: 195-204.

Ross, C.S. and Smith, R.L., 1961. Ash-low tuffs: their origin, geologic relations and identifications. U.S. Geol. Survey Prof. paper 366: 1-177.

Saemundsson, K., 1974. Evolution of the axial rifting zone in northern Iceland and the Tjörnes fracture zone. Geol. Soc. Amer. Bull., 85: 495-504.

Saemundsson, K., 1978. Fissure swarms and central volcanoes of the neovolcanic zones, Iceland. Geol. J. special issue 10: 415-432.

Saemundsson, K., 1979. Outline of the Geology of Iceland. Jökull, 26: 7-27.

Saemundsson, K., 1982. Öskjur virkum eldfjallasvaedum a Islandi (Calderas within the volcanic zones of Iceland). In: H. Thorarinsdottir, O.H. Oskarsson, S. Steinthorsson and Th. Einarsson (Editor), Eldur er i Nordri. Sögufelag, Reykjavik, pp 224-226.

Schmincke, H.-U. and Swanson, D.A., 1967. Laminar viscous flowage structures in ash-flow tuff from Gran Canaria, Canary Islands. J. Geol. 75: 641-664.

Sigurdsson, H., and Sparks, R.S.J., 1981. Petrology of rhyolitic and mixed magma from the 1875 eruption of Askja, Iceland. J. Petrology, 22: 41-84.

Sigvaldason, G., 1979. Rifting magmatic activity and interaction between acid and basic liquids: the 1875 Askja eruption in Iceland. Nordic Volcanological Institute report 7903: 1-54.

Sparks, S.R.J., Sigurdsson, H., and Wilson, L., 1977. Magma mixing: a mechanism for triggering acid explosive eruptions. Nature, 267: 315-318.

Sparks, R.S.J., and Pinkerton, H., 1978. Effects of degassing on the rheology of basaltic magma. Nature, 276: 385-386.

Sparks, R.S.J., and Wright, J.V., 1979. Welded air-fall tuffs. In: C.E. Chapin and W.E. Elston (Editors), 1979. Ash Flow Tuffs. Geol. Soc. Amer. special paper 180, pp 155-166.

Walker, G.P.L. and Croasdale, R., 1972. Characteristic of some basaltic pyroclastics. Bull. Volcanol., 35: 303-312.

Walker, G.P.L., 1981. Plinian eruptions and their products. Bull. Volcanol., 44: 223-240.

Walker, G.P.L., Self, S. and Wilson, L., 1984. Tarawera, 1886, New Zealand -a basaltic plinian fissure eruption. J. Volcanol. Geotherm. Res., 21: 61-78.

Williams, S.N., 1983. Plinian air-fall deposits of basaltic compositions. Geology, 11: 211-214.

Wolff, J.A., and Wright, J.V., 1981. Rheomorphism of welded tuffs. J. Volcanol. Geotherm. Res., 10: 13-34.

Wolff, J.A. and Wright, J.V., 1982. Formation of the Green Tuff, Pantelleria. Bull. Volcanol., 44: 681-690.

Wright, J.V., Smith, A.L. and Self, S., 1980. A working terminalogy of pyroclastic deposits. J. Volcanol. Geotherm. Res., 8: 315-336.

TABLE 1

Iron Titration Data

Sample (Location)	Fe0	Fe203	Fe203/Fe0
A-1a (NH)	3.82	0.75	0.19
A-1 (NH)	6.63	0.25	0.03
A-3 (Hl)	2.82	4.68	1.65
B-1 (NH)	3.65	6.50	3.42
B-11 (NH)	4.10	9.57	2.33
C-11 (NH)	5.60	2.12	0.37
C-14 (WH)	4.11	4.15	1.00
D-14 (SH)	3.23	5.28	1.60
D-19 (EH)	1.07	11.66	10.89
D-10 (NH)	8.77	11.36	1.29
D-20 (SH)	1.83	10.77	5.80
E-18 (EH)	12.55	0.76	0.08
E-19 (EH)	7.74	2.44	0.13
E-15 (EH)	9.84	2.18	0.22

TABLE 2

Volume calculations and DRE volumes for each of the units of the Krafla Layer.

Unit	A	B	C	D	E	Total
Glass density (g/cm3)	2.52	2.88	2.56	2.79	2.79	
Si02 (wgt. %)	69	51	66	59	61	
Void space (%)	68	29	1	11	8	
Thickness (m)	0.90	1.00	0.68	20	5.00	
Area (km3)	84	84	84	101	101	
Volume (km3)	0.076	0.084	0.057	2.020	0.505	
DRE (km3)	0.025	0.060	0.056	1.797	0.460	2.85
Lithics (%)	0.30	2.00	1.00	3.00	3.00	

Glass densities are based on silica content for each of the units.
Lithic percentages are based on point counting techniques.
Silica values are from table 3 in this report.
Area values for each of the units are approximated from the isopach m showing the distribution of the units (figure 9).

TABLE 3

Whole rock compositions and CIPW norm calculations for selected unit s

Sample	A-1a	A3	A1	B1	B11	C11	D14	E18
Si02	69.53	67.83	68.14	50.92	52.88	66.47	59.93	61.45
Ti02	00.90	00.80	00.51	02.15	02.15	01.10	01.83	01.36
Al203	11.42	12.62	10.91	14.87	13.58	12.41	12.65	12.62
Fe203	00.76	04.68	00.25	12.50	09.57	02.12	05.28	02.44
FeO	03.82	02.82	06.63	03.65	04.10	05.60	03.23	07.74
MnO	00.79	00.70	00.88	00.19	00.21	00.12	00.16	00.16
MgO	01.03	02.40	01.33	04.09	04.33	01.95	03.40	02.36
CaO	03.60	04.60	03.07	09.03	10.01	04.66	06.33	05.34
Na20	03.09	01.59	03.34	02.49	02.54	03.80	02.79	03.01
K20	01.90	01.44	01.89	00.74	00.52	01.19	01.38	01.45
P205	00.03	00.00	00.11	00.25	00.28	00.10	00.30	00.19
Total	97.16	99.48	97.06	100.88	100.17	99.52	97.28	98.12
CIPW								
AN	31.03	62.91	24.55	56.36	52.88	29.25	43.15	39.52
Q	33.24	36.36	28.56	05.42	09.05	26.02	21.45	21.16
Or	11.23	08.51	11.17	04.37	03.07	07.03	08.16	08.57
Ab	26.05	13.45	28.26	21.07	21.49	32.15	23.61	25.47
An	11.73	22.82	09.20	27.21	24.12	13.29	17.92	16.64
C	00.00	00.08	00.00	00.00	00.00	00.00	00.00	00.00
Di	06.33	00.00	04.59	13.38	19.64	07.68	09.30	07.26
Hy	05.70	13.17	13.17	18.59	12.18	07.94	07.66	12.46
Mt	01.10	03.33	00.36	05.29	05.29	03.07	04.83	02.58
Il	01.71	01.52	00.97	04.08	04.08	02.09	03.48	02.58
Ap	00.07	00.00	00.25	00.58	00.65	00.23	00.70	00.44
FeO(t)	04.50	07.03	06.86	14.60	12.71	07.51	07.98	09.94
F/F+M	0.837	0.763	0.853	0.787	0.749	0.796	0.705	0.811
Density	02.42	02.45	02.45	02.60	02.60	02.47	02.50	02.52

The above data were obtained by the following methods: Si02, Al203, Ti Fe203 (total) CaO, K20 by X-ray fluorescence; MnO, MgO and Na20 by ato absorption; P205 by spectrophotometry and FeO by titration techniques. The CIPW normative values are based on the scheme outlined by Irvine a Baragar, 1971.

TABLE 4

Glass compositions.

	ACID	BASIC	INTERMEDIATE
Unit	A1	B10	E19
Si02	73.11	51.15	50.34
Al203	11.80	12.70	12.95
Ti02	00.25	01.93	02.73
Fe0	03.00	10.04	14.83
Mn0	00.10	00.20	00.30
Mg0	00.11	07.19	05.00
Ca0	01.75	13.21	09.94
Na20	04.23	03.91	03.31
K20	02.66	00.39	00.39
P205	00.10	00.19	00.26
Total	97.00	98.99	100.03

note: Intermediate units host mixed glassed compositions similar to bo acid and basic unit compositions.

TABLE 5

Plagioclase mineral analyses used in least squares modeling (Bryan, W.B.,Finger, L.W. and Cheayes, F., 1969) for selected unit samples. The following tables consist of eight analyses for each of the five units. Data obtained by electron microscope anal in appendix 1 of this report.

Sample	A1	A2	A3	A4	A5	A6	A7	A8
Si02	53.86	48.65	58.28	54.00	46.94	45.42	46.51	46.55
Al203	30.06	33.83	26.32	30.07	33.66	34.47	33.83	31.45
Fe0	00.84	00.46	00.84	00.94	00.56	00.52	00.47	00.48
Ca0	13.24	17.05	08.87	13.27	16.58	17.44	17.01	17.32
Na20	03.93	01.45	05.94	04.40	01.76	01.07	01.33	01.25
K20	00.09	00.02	00.24	00.08	00.02	00.07	00.02	00.02
Fe0(t)	00.84	00.46	00.84	00.95	00.56	00.52	00.47	00.48
Total	102.02	101.46	100.49	102.77	99.52	98.99	99.16	99.07
density	2.50	2.55	2.44	2.50	2.55	2.56	2.55	2.56

Sample	B1	B2	B3	B4	B5	B6	B7	B8
Si02	50.00	49.54	51.09	44.78	49.99	50.81	50.55	50.58
Al203	31.54	33.01	31.99	36.05	32.84	31.92	31.43	31.95
Fe0	00.85	00.98	00.79	00.70	00.82	00.79	00.74	00.75
Ca0	13.36	14.49	13.41	17.51	14.16	14.88	15.42	14.00
Na20	04.20	03.63	04.21	01.86	03.27	03.26	03.27	03.36
K20	00.11	00.13	00.06	00.00	00.12	00.17	00.00	00.10
Fe0(t)	00.85	00.98	00.79	00.70	00.82	00.79	00.74	00.75
Total	100.06	101.78	101.55	100.90	101.20	101.83	101.41	100.74
density	2.51	2.52	2.51	2.57	2.52	2.52	2.52	2.51

Sample	C1	C2	C3	C4	C5	C6	C7	C8
Si02	50.18	52.74	48.06	52.04	53.84	51.29	49.29	48.92
Al203	29.21	32.14	29.12	31.96	32.11	33.50	33.99	31.95
Fe0	0.42	00.85	00.56	00.76	01.05	00.63	00.72	00.76
Ca0	11.97	13.51	11.77	13.12	12.34	15.12	15.18	14.96
Na20	04.69	03.92	05.06	04.00	03.81	02.88	02.85	03.00
K20	00.22	00.09	00.16	00.90	00.09	00.01	00.08	00.05
Fe0(t)	00.42	00.85	00.56	00.76	01.05	00.63	00.72	00.76
Total	98.69	103.26	94.73	102.78	103.24	103.43	102.11	99.64
density	2.48	2.50	2.49	2.50	2.50	2.52	2.53	2.53

Sample	D1	D2	D3	D4	D5	D6	D7	D8
Si20	50.10	52.64	51.30	50.91	49.20	46.59	47.17	48.93
Al203	32.52	29.33	32.74	33.17	34.13	33.97	35.17	34.97
Fe0	00.82	00.44	00.60	00.70	00.72	00.56	00.47	00.56
Ca0	14.84	15.83	17.46	15.39	16.01	16.57	17.98	16.95
Na20	01.51	01.27	01.30	02.65	02.16	01.66	01.32	01.56
K20	00.29	00.06	00.07	00.11	00.05	00.06	00.05	00.07
Fe0	00.82	00.44	00.60	00.70	00.72	00.56	00.47	00.56

Sample	D1	D2	D3	D4	D5	D6	D7	D8
Si20	50.10	52.64	51.30	50.91	49.20	46.59	47.17	48.93
Al203	32.52	29.33	32.74	33.17	34.13	33.97	35.17	34.97
Fe0	00.82	00.44	00.60	00.70	00.72	00.56	00.47	00.56
Ca0	14.84	15.83	17.46	15.39	16.01	16.57	17.98	16.95
Na20	01.51	01.27	01.30	02.65	02.16	01.66	01.32	01.56
K20	00.29	00.06	00.07	00.11	00.05	00.06	00.05	00.07
Fe0	00.82	00.44	00.60	00.70	00.72	00.56	00.47	00.56
Total	100.08	99.57	103.47	102.93	102.27	99.41	102.81	103.04
density	2.53	2.52	2.54	2.53	2.54	2.55	2.56	2.55

Sample	E1	E2	E3	E4	E5	E6	E7	E8
Si20	46.52	49.07	49.07	48.96	54.33	49.32	46.54	53.70
Al203	33.77	33.70	33.70	32.85	30.80	33.65	33.34	31.11
Fe0	00.61	00.59	00.59	00.61	00.86	00.46	00.52	00.87
Ca0	17.93	16.50	16.85	16.42	12.34	16.84	16.97	13.55
Na20	01.26	01.74	01.80	01.82	03.95	01.60	01.41	03.73
K20	00.03	00.05	00.05	00.11	01.10	00.03	00.03	00.10
Fe0(t)	00.61	00.59	00.59	00.61	00.86	00.46	00.52	00.87
Total	100.12	101.65	102.06	100.77	102.38	101.90	98.81	103.06
density	2.56	2.54	2.54	2.54	2.49	2.54	2.55	2.50

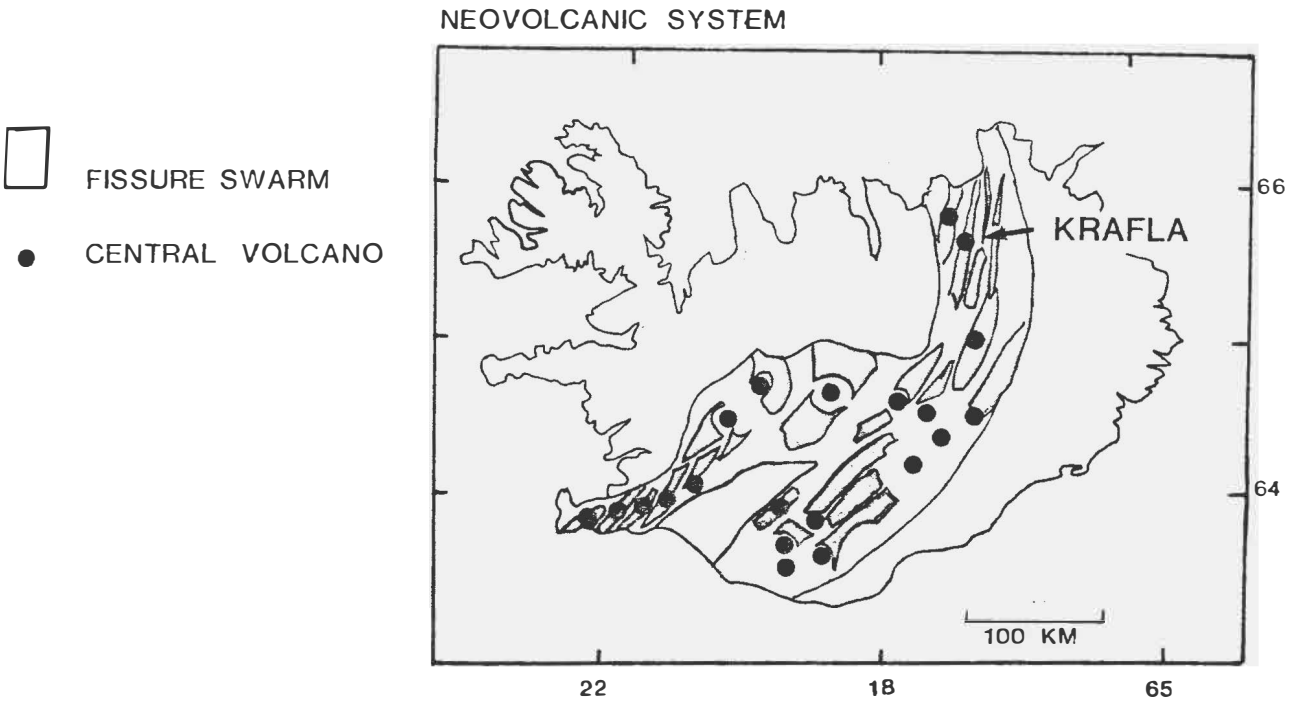

Figure 1. Location map of the Krafla volcanic center, northern Iceland.

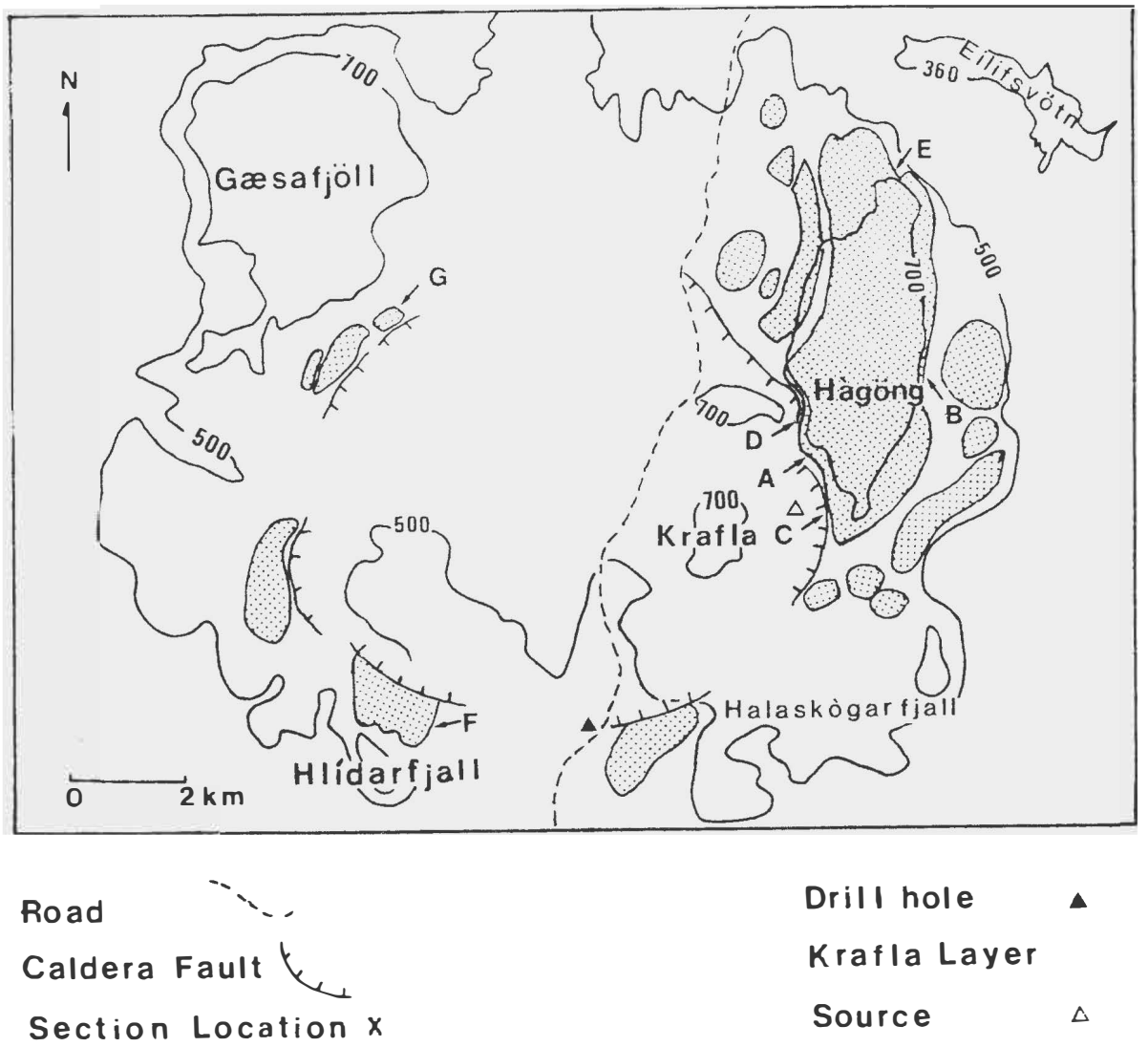

Figure 2. Geological map showing the distribution of the Krafla air-fall Layer and the proximity to the caldera faults. Contour lines at 500 and 700 meter elevations. Letters refer to sections in figure 4a and b. Section A: 60 m length, traverse direction N35W. Section B: 40 m length, traverse direction N3E. Section C: 50 m length, traverse direction N35W. Section D: 60 m length, traverse direction N10W. Section E: 40 m length, traverse direction N70W. Section F: 60 m length, traverse direction N5E. Section G: 30 m length, traverse direction N35E.

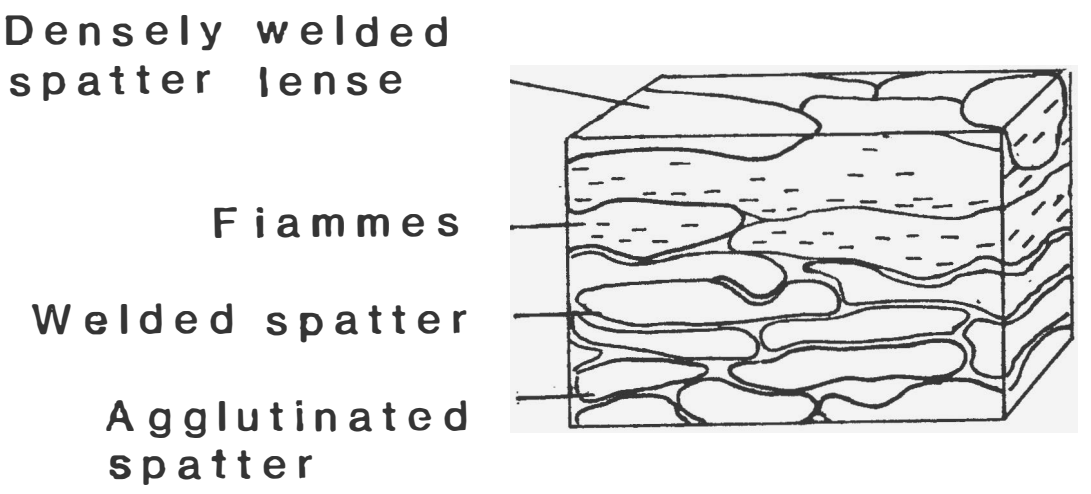

Figure 3. Schematic block diagram of the welding characteristics of the Krafla Layer.

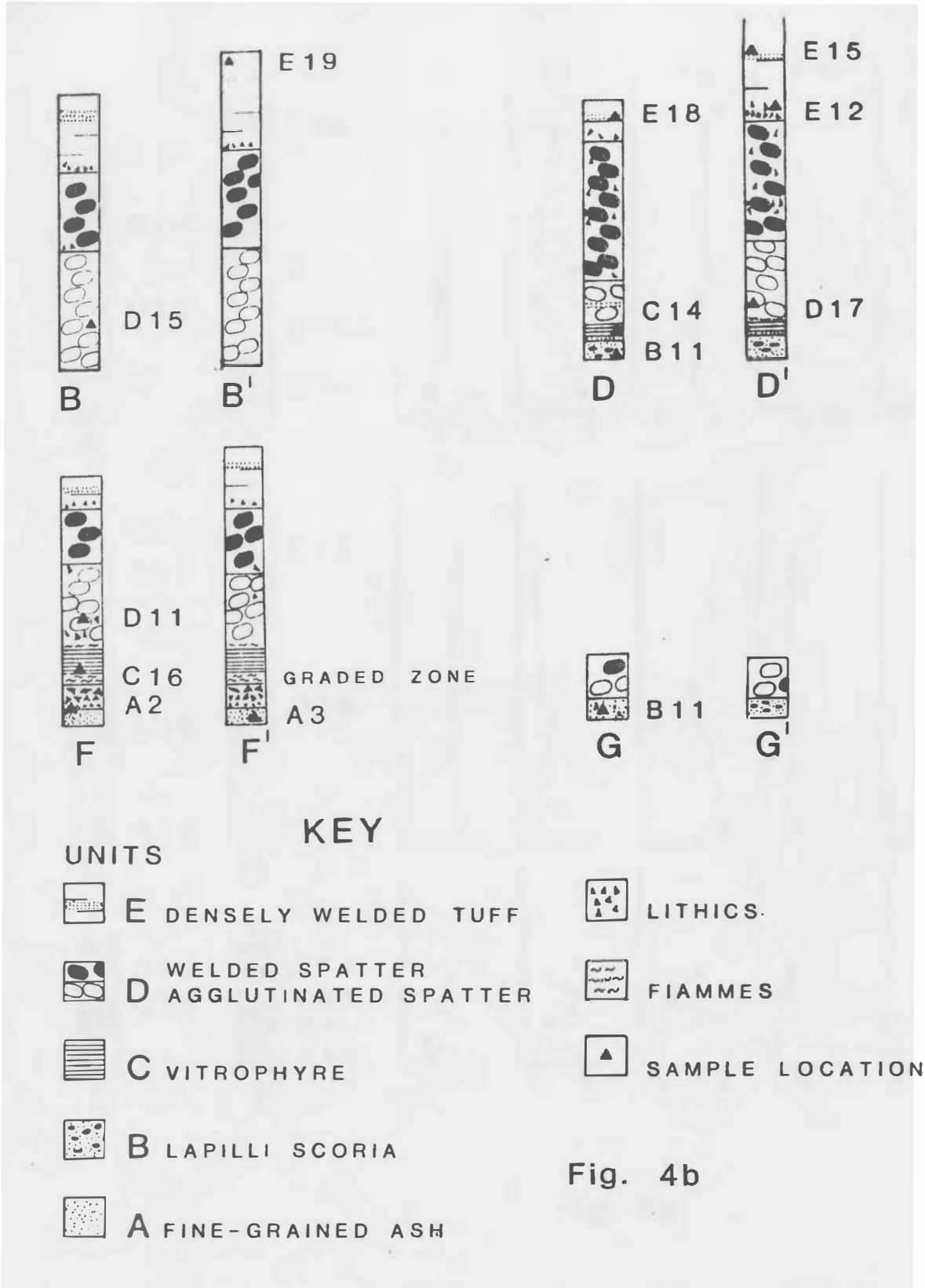

Fig. 4b

Figure 4a and 4b. Stratigraphic sections selected to show the distribution of the five unit facies and the general major-oxide variation for the continuously sampled sections. Scale: 1cm is 6m. SD = median spatter size (the average of 20 measurments of the long axis in cm); LD = median lithic size (the average of 5 measurements of the long axis in cm). FR = flattening ratio of an average of 20 fiammes. Section A: SD = 41, LD = 19, FR = 1:24. Section B: SD = 37, LD = 14, FR = 1:21. Section C: SD = 34, LD = 14, FR = 1:19. Section D: SD = 47, LD = 55, FR = 1:19. Section E: SD = 55, LD = 15, FR = 1:22. Section F: SD = 57, LD = 28, FR = 1:15. Section G: SD = 25, LD = 14, FR = 1:9. Oxide variation data obtained by atomic absorption techniques.

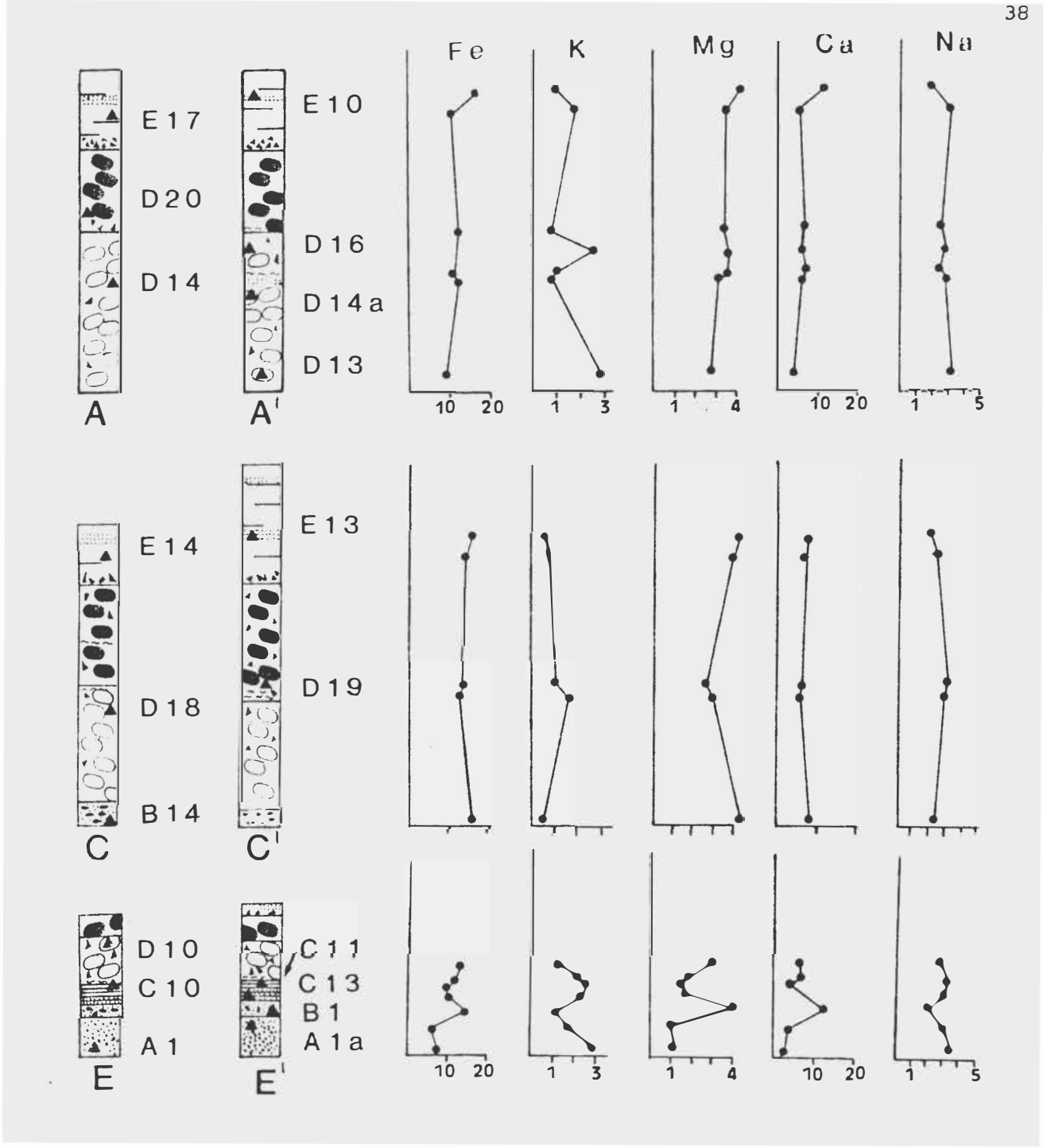
Fe
K
Mg
Ca
Na
E17
D20
D14
A
E10
D16
D14a
D13
A'
10 20
1 3
1 4
10 20
1 5
E14
D18
B14
C
E13
D19
C'
D10
C10
A1
E
C11
C13
B1
A1a
E'

Fig. 4a

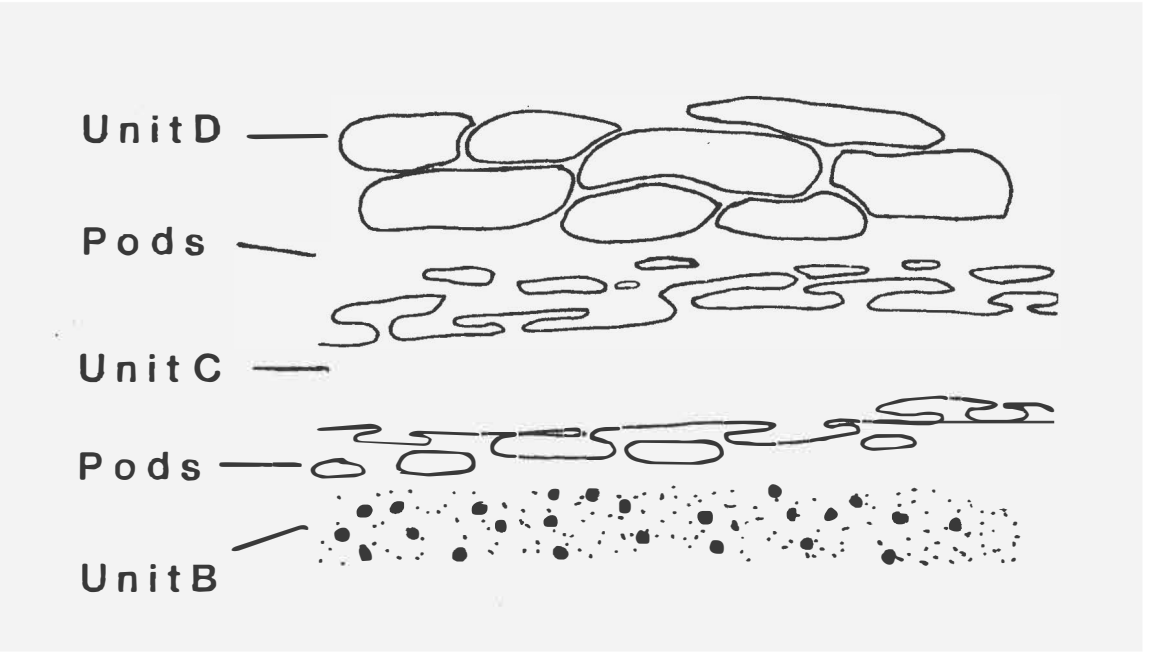

Figure 5. Diagram of the podding nature of the vitrophyre unit C.

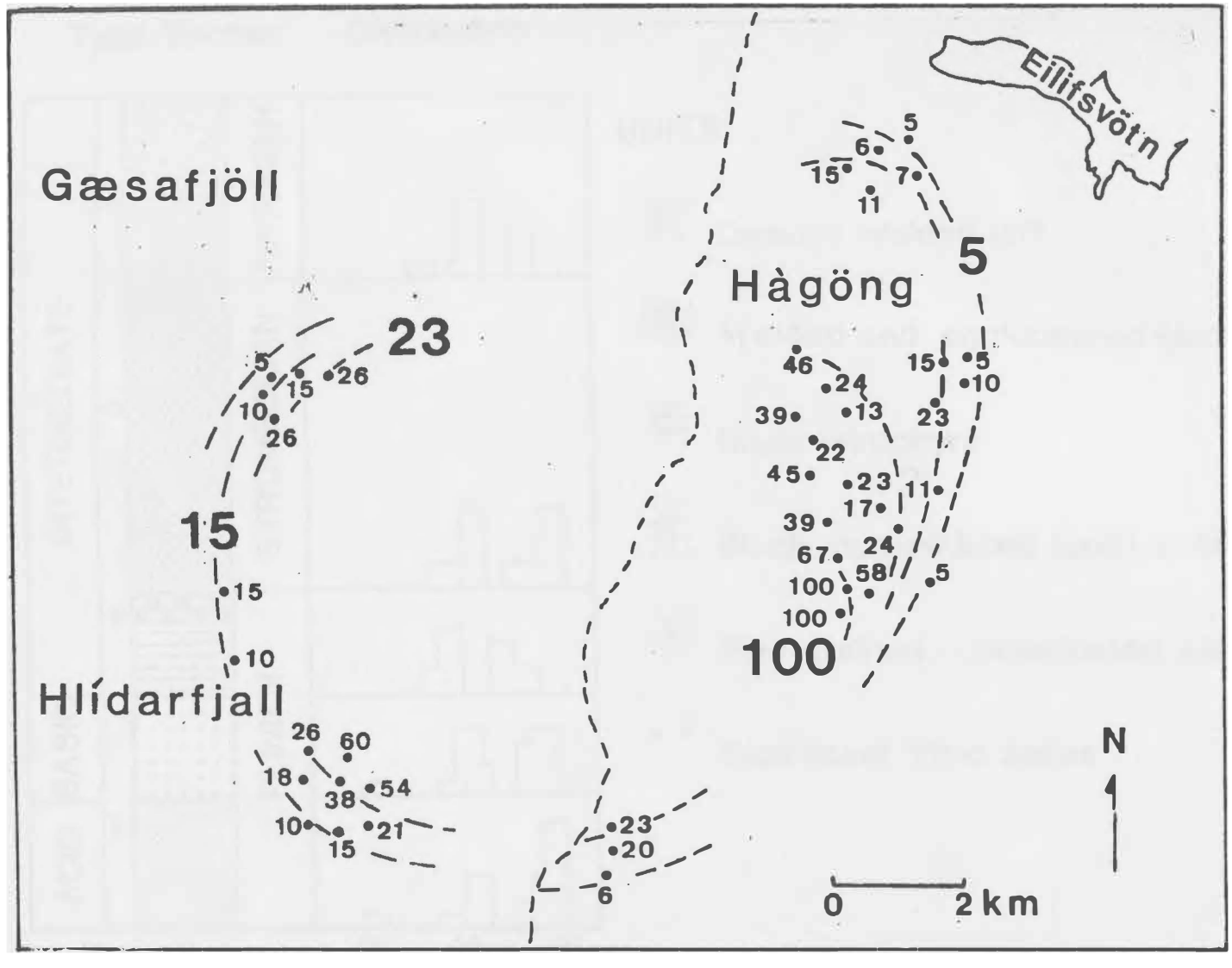

Figure 6. Isopleth map for the median lithic diameter distribution for the welded spatter unit D. Each point represents the average length of 5 lithic fragments in cm.

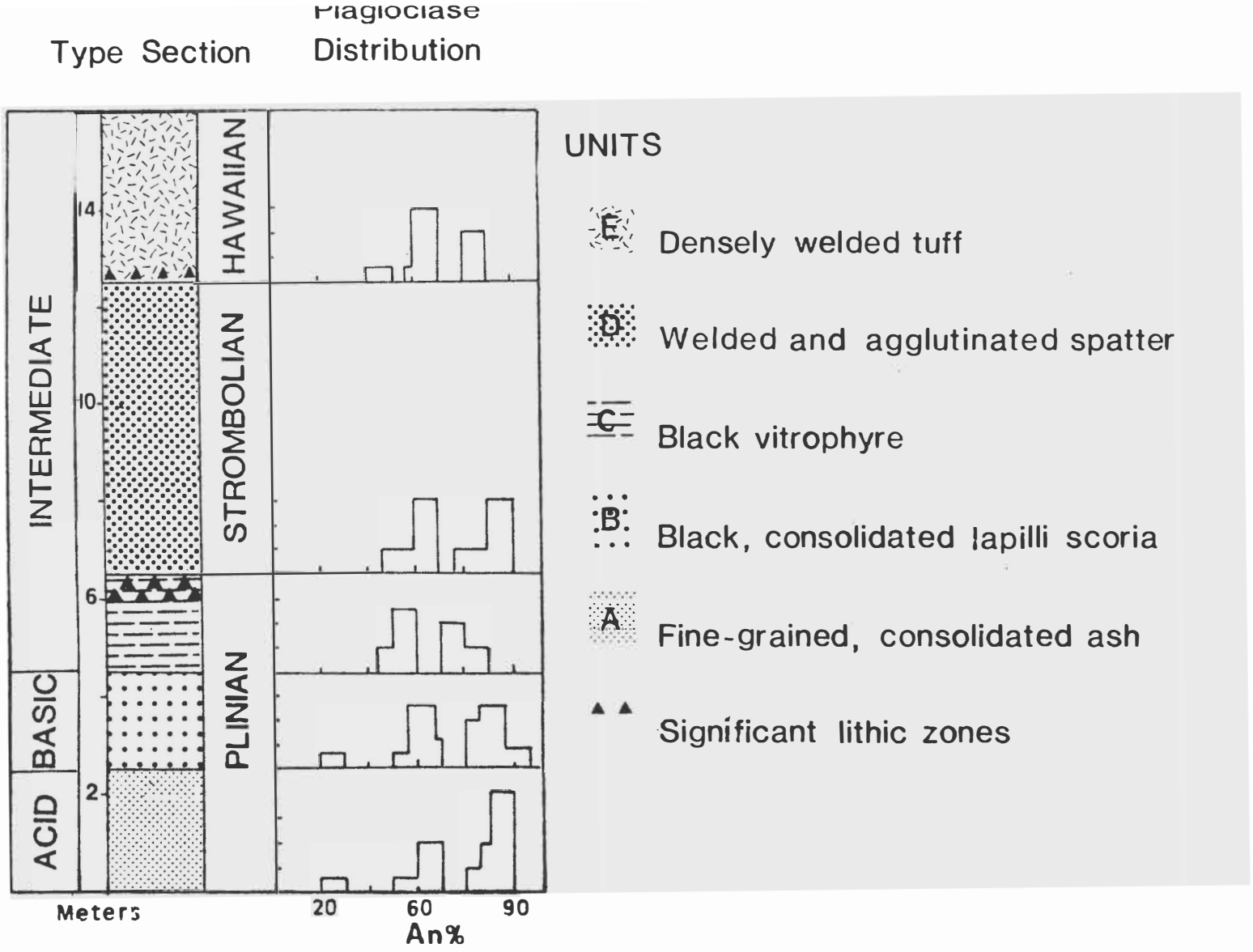

Figure 8. A schematic diagram of a typical section and the corresponding degree of welding for each of the units. The plagioclase histograms show a bimodal composition The units host both sodic and calcic plagioclase populations.

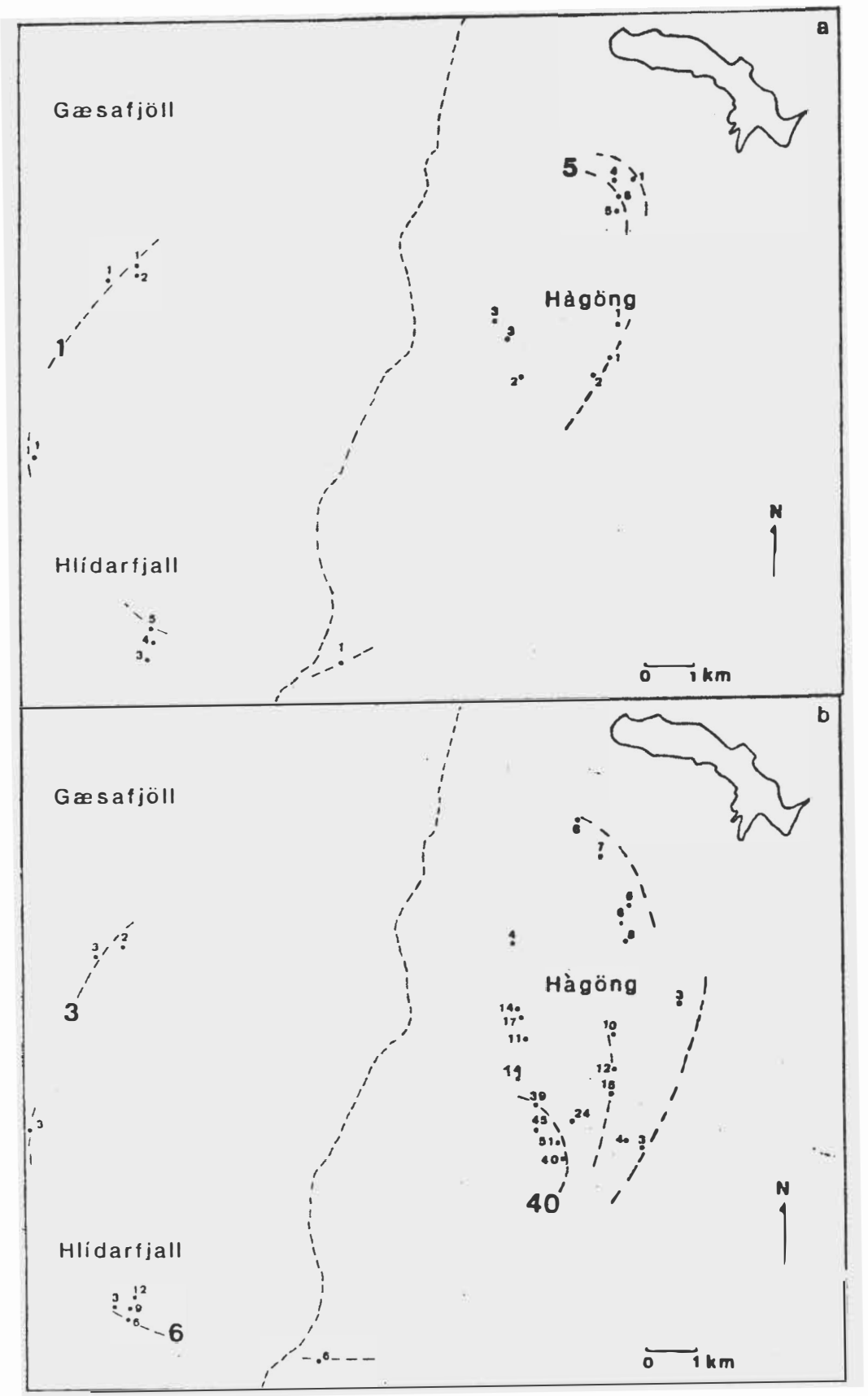

Figure 9. Thickness isopach diagrams (in meters) for both the Plinian phase (upper map a) and the Strombolian-Hawaiian phase (lower map b) of the eruption. Thickness measurements for units A, B and C were used to construct map 9a and units D and E were used to construct map 9b.

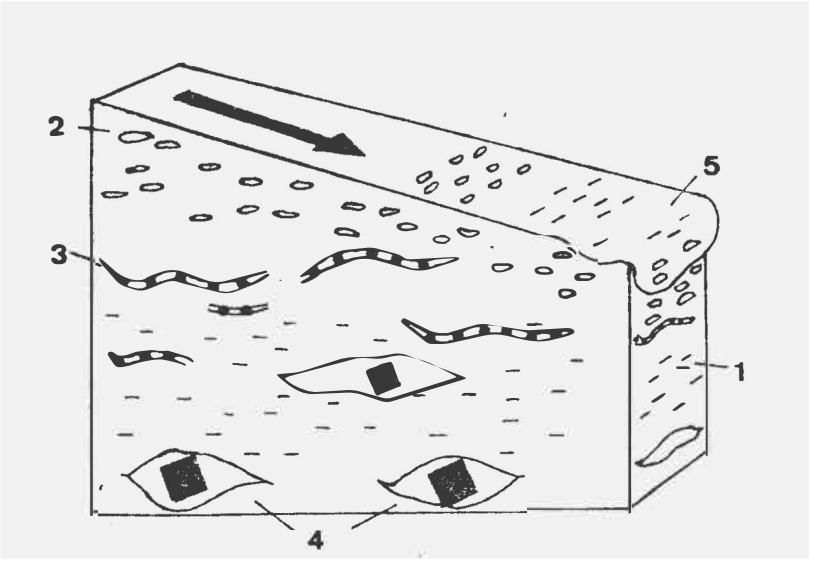

1, Stretched and flattened fiamme zone (unitD).

2, Stretched and flattened vesicles (unitE)

3, Flow veins with lithic fragments (unitD)

4, Spindle shaped voids unitD.

5, Downslope flow feature of the upper densely welded unitE.

Figure 7. Block diagram of the flow features of the Krafla welded units.

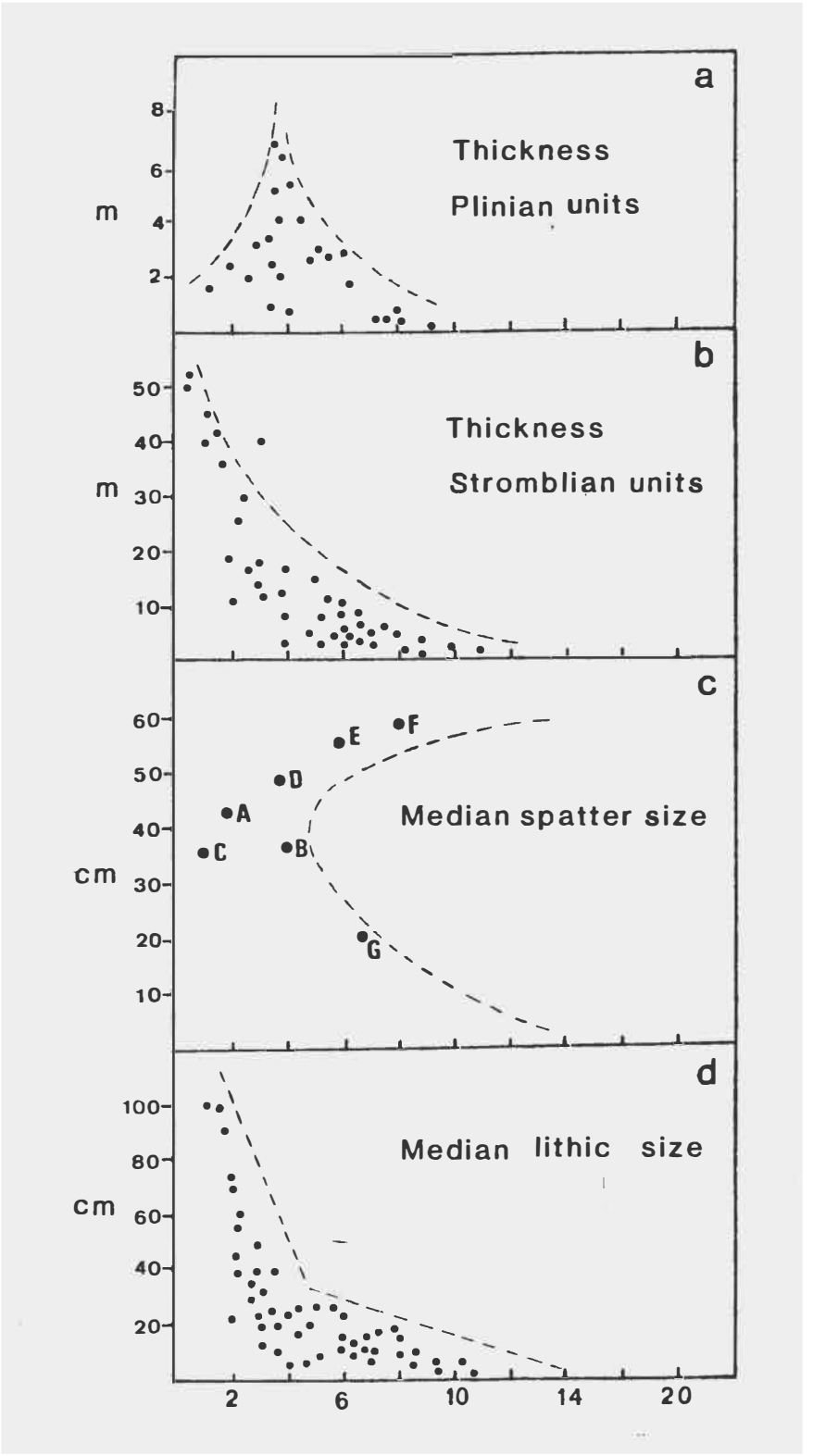

Figure 10. Diagram modeling the tephra sizes and thickness distributions for Strombolian and Plinian phases verses the distance from the plausible source locality (figure 2), which is in the southeast of the present caldera, to the east of Krafla mountain. Data in diagram c and d are from unit D, the welded spatter unit. Each point in diagram c is the average of 20 measurements. Each point in diagram d is the average of 5 measurements.

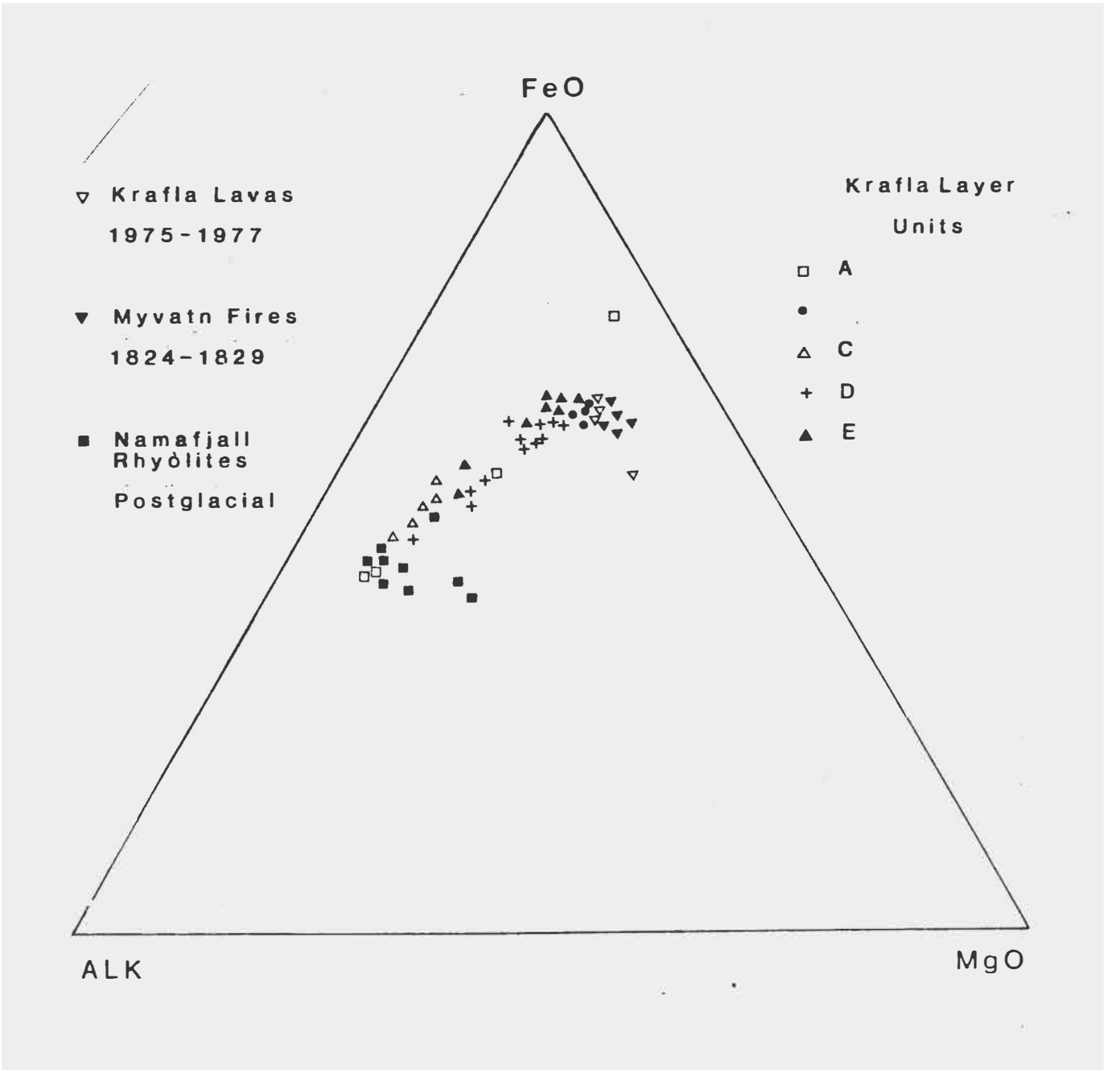

Figure 11. AMF diagram showing the typical tholeiitic trend for Icelandic rock suites. Compositions plotted show the similarities between the acid unit in the Krafla Layer and Namafjall Rhyolite compositions. Unit B, the most basic tephra in the Krafla Layer, plots in close proximity to the recent tholeiitic lava flows. Data was obtained by atomic absorption techniques. Comparative data supplied by Grönvold, 1972, p.177 (Namafjall analyses); Grönvold, 1978, p.7 (Krafla Fire Analyses); and Grönvold, 1984, p.10 (Myvatn analyses).

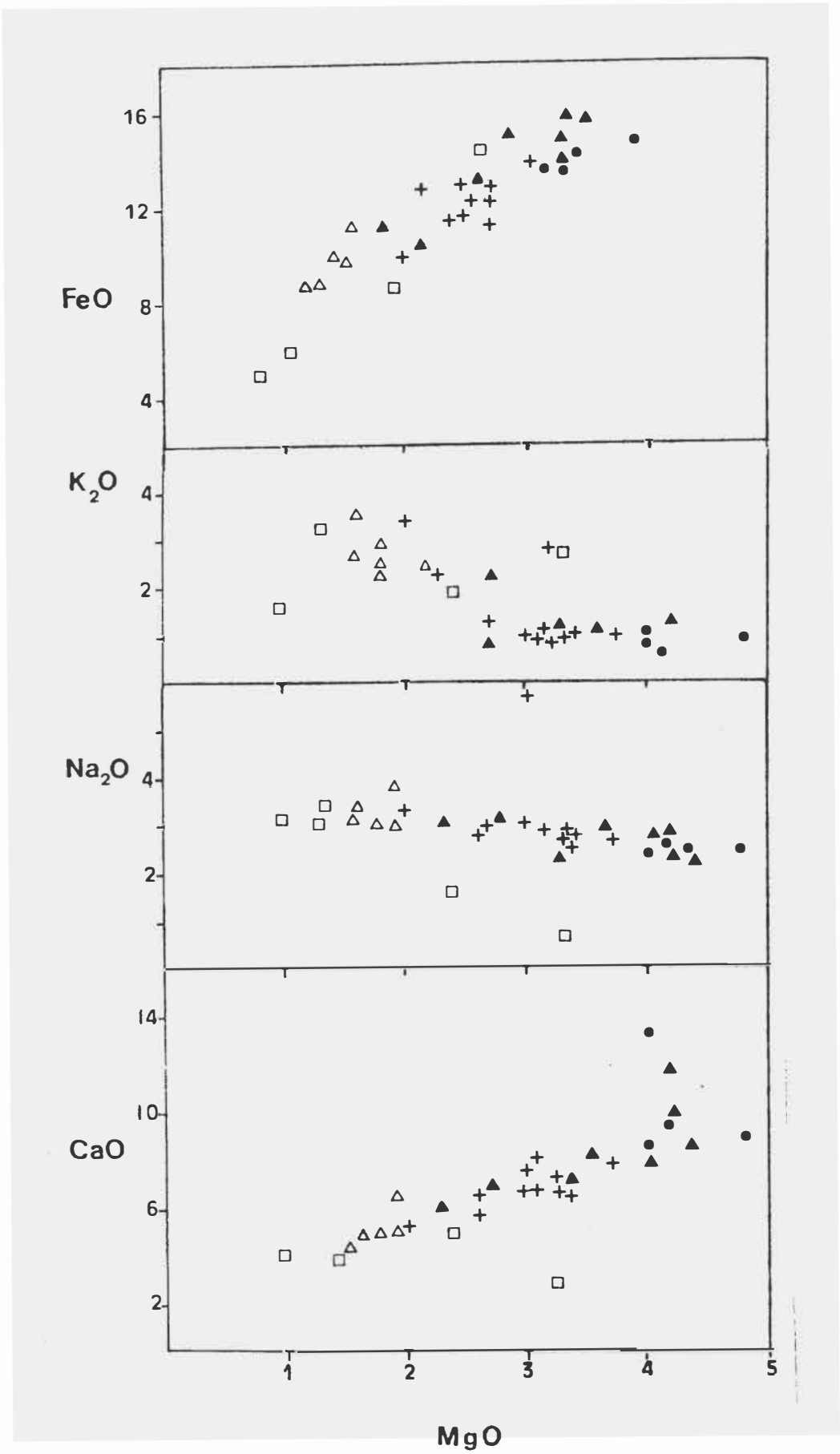

Figure 12. Major-elements of the Krafla units plotted against MgO. Data obtained by atomic absorption techniques.

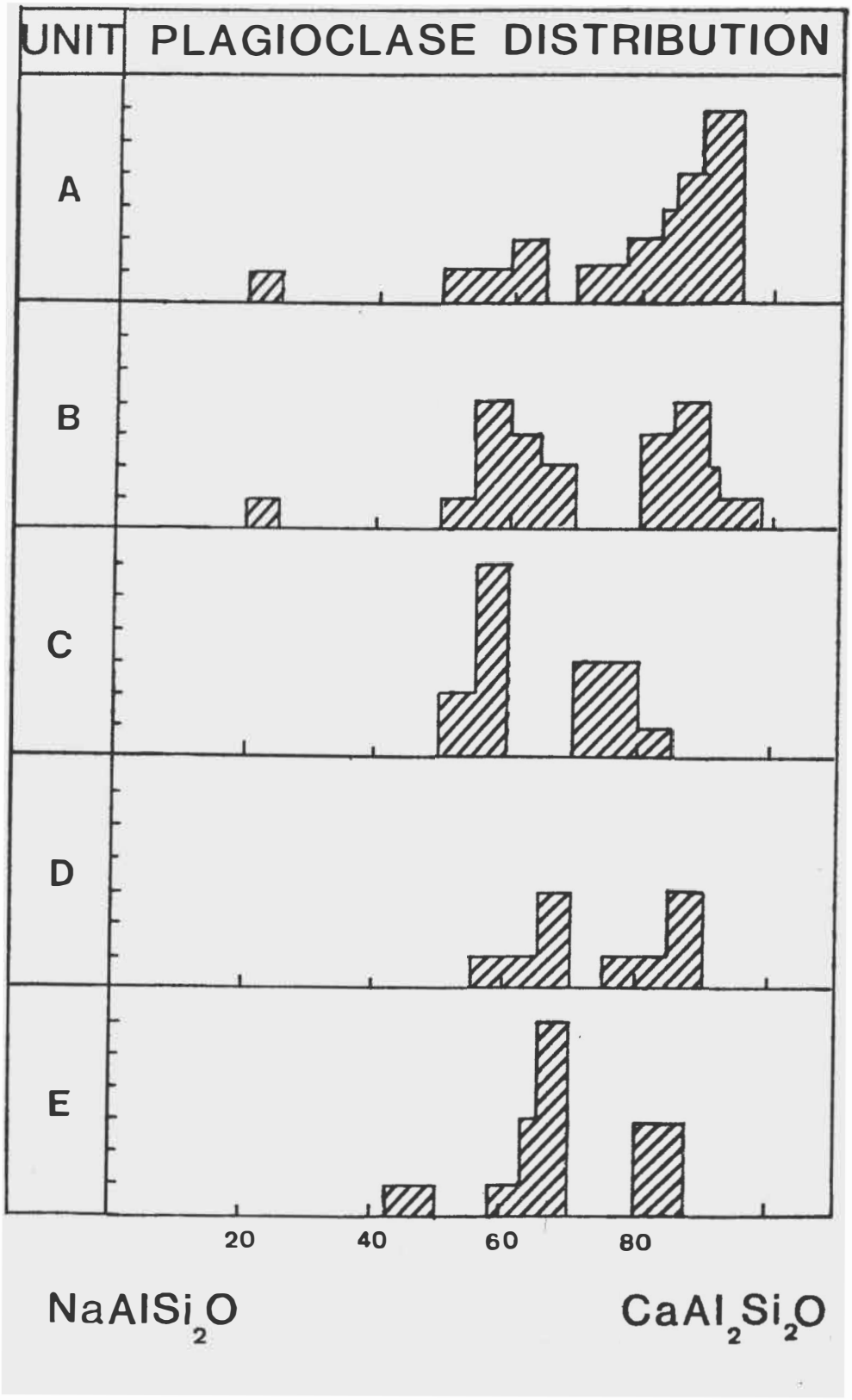

Figure 13. Plagioclase composition histograms for each of the five air-fall units. Data was obtained by electron microprobe techniques.

APPENDIX 1

Microprobe analyses for the air-fall unit.
Section 1: Plagioclase analyses.

Unit A
PLAGIOCLASE ANALYSIS
numbers based on weight percents

	1	2	3	4	5	6	7	8
SiO2	53.86	48.65	58.28	55.01	46.94	45.42	46.51	46.55
Al203	30.06	33.83	26.32	30.07	33.66	34.47	33.83	33.45
FeO(t)	00.84	00.46	00.84	00.95	00.56	00.52	00.47	00.48
CaO	13.24	17.05	08.87	13.27	16.58	17.44	17.01	17.32
Na20	03.93	01.45	05.94	04.40	01.76	01.07	01.32	01.32
K20	00.09	00.02	00.24	00.08	00.02	00.07	00.02	00.02
Total	102.00	101.06	100.09	103.07	99.05	99.02	98.09	99.07

note: Plagioclase microprobe analyses performed on magnetically separated samples.

Unit A
numbers of ions on the basis of 8 oxygen

Si	2.399	2.196	2.601	2.411	2.166	2.113	2.154	2.116
Al	1.578	1.001	1.385	1.554	1.831	1.890	1.847	1.830
Fe	0.031	0.017	0.031	0.035	0.022	0.020	0.018	0.019
Ca	0.632	0.825	0.424	0.623	0.820	0.869	0.844	0.867
Na	0.339	0.127	0.514	0.374	0.157	0.096	0.119	0.112
K	0.005	0.001	0.014	0.004	0.005	0.004	0.001	0.001
An	64.75	86.56	44.53	62.23	83.50	89.68	87.55	88.39
Ab	34.73	13.32	53.99	37.36	15.98	09.90	12.30	11.49
Or	00.51	00.10	01.47	00.40	00.50	00.41	00.10	00.10

Basic unit:

Unit B
PLAGIOCLASE ANALYSES
numbers in weight percent

	1	2	3	4	5	6	7	8
Si02	50.00	49.54	51.09	44.78	49.99	50.81	50.55	50.58
Al203	31.54	33.01	31.99	36.05	32.84	31.92	31.43	31.95
Fe0	00.85	00.98	00.79	00.70	00.82	00.79	00.74	00.75
Ca0	13.36	14.49	13.41	17.51	14.16	14.88	15.42	14.00
Na20	04.20	03.63	04.21	01.86	03.27	03.26	03.27	03.36
K20	00.11	00.13	00.06	00.00	00.12	00.17	00.05	00.10
Total	100.06	101.36	101.55	100.89	102.68	101.83	101.40	100.56

Unit B
number of ions on the basis of 8 oxygen

Si	2.380	2.234	2.297	2.139	2.257	2.278	2.295	2.291
Al	1.609	1.755	1.696	1.863	1.748	1.725	1.724	1.706
Fe	0.031	0.037	0.030	0.026	0.031	0.028	0.026	0.028
Ca	0.619	0.700	0.646	0.823	0.685	0.688	0.702	0.679
Na	0.352	0.317	0.367	0.158	0.286	0.273	0.269	0.295
K	0.000	0.007	0.003	0.000	0.007	0.009	0.003	0.007
An	63.74	68.35	63.58	83.89	70.04	70.92	72.07	69.21
Ab	36.24	30.95	36.12	16.10	29.24.	28.14	27.61	30.07
Or	00.00	00.68	00.29	00.00	00.71	00.92	00.31	00.71

Intermediate units:

Unit C
PLAGIOCLASE ANALYSES
number based on weight percent

	1	2	3	4	5	6	7	8
SiO	52.18	48.06	52.74	52.04	53.84	51.29	49.29	48.92
Al203	29.21	29.12	32.14	31.96	32.11	33.50	33.99	31.95
FeO	00.42	00.56	00.85	00.76	01.05	00.63	00.72	00.76
CaO	11.97	11.77	13.51	13.12	12.34	15.12	15.18	14.96
NaO	04.96	05.06	03.92	04.00	03.81	02.88	02.85	03.00
K20	00.22	00.16	00.09	00.09	00.09	00.01	00.08	00.05
Total	99.09	94.83	103.25	101.97	104.27	103.43	102.11	99.63

Unit C
number of ions on the basis of 8 oxygen

Si	2.396	2.320	2.316	2.333	2.349	2.263	2.211	2.250
Al	1.581	1.681	1.671	1.682	1.651	1.742	1.797	1.732
Fe	0.020	0.023	0.031	0.028	0.038	0.023	0.027	0.029
Ca	0.589	0.609	0.639	0.628	0.624	0.715	0.730	0.737
Na	0.442	0.474	0.335	0.346	0.322	0.246	0.248	0.268
K	0.013	0.010	0.005	0.005	0.005	0.000	0.005	0.003
An	56.41	55.71	65.27	64.14	65.61	74.40	74.26	73.11
Ab	42.33	43.36	34.21	35.34	33.85	25.59	25.22	26.58
Or	01.24	00.91	00.51	00.51	00.52	00.00	00.50	00.29

Unit D
PLAGIOCLASE ANALYSES
numbers based on weight percent

	1	2	3	4	5	6	7	8
Si02	50.10	52.64	51.30	50.91	49.20	46.59	47.17	48.93
Al203	32.52	29.33	32.74	33.17	34.13	33.97	35.82	34.97
Fe0	00.82	00.44	00.60	00.70	00.72	00.56	00.47	00.57
Ca0	14.84	15.83	17.46	15.39	16.01	16.57	17.98	16.95
Na20	01.51	01.27	01.30	02.65	02.16	01.66	01.32	01.56
K20	00.29	00.06	00.07	00.11	00.05	00.06	00.05	00.07
Total	99.86	99.57	101.47	102.93	102.30	99.43	101.05	101.05

Unit D
number of ions on the bases of 8 oxygen

Si	2.430	2.236	2.2677	2.260	2.202	2.153	2.112	?.176
Al	1.504	1.732	1.706	1.736	1.802	1.851	1.891	1.833
Fe	0.033	0.018	0.022	0.026	0.027	0.022	0.018	0.021
Ca	0.771	0.849	0.827	0.732	0.768	0.820	0.863	0.808
Na	0.143	0.123	0.111	0.228	0.188	0.149	0.115	0.135
K	0.018	0.004	0.004	0.006	0.003	0.004	0.003	0.004
An	83.53	87.81	85.54	75.77	80.81	85.07	88.81	86.08
Ab	15.38	12.72	11.48	23.60	19.78	15.45	11.83	14.06
Or	01.95	00.41	00.41	00.62	00.31	00.41	00.30	00.42

Note: the above analyses are from several points from unit D thinsections.

Unit E
PLAGIOCLASE ANALYSES
numbers in weight percent

	1	2	3	4	5	6	7	8
Si02	46.52	49.07	49.07	48.96	54.33	49.32	46.54	53.70
Al203	33.77	33.70	33.70	32.85	30.80	33.65	33.34	31.11
Fe0	00.61	00.59	00.59	00.61	00.86	00.46	00.52	00.87
Ca0	17.93	16.85	16.85	16.42	12.34	16.84	16.97	13.55
Na20	01.26	01.74	01.80	01.82	03.95	01.60	01.41	03.73
K20	00.03	00.05	00.05	00.11	00.10	00.03	00.03	00.10
Total	100.93	101.99	102.06	100.77	102.38	101.91	98.81	103.00

Unit E
number of ions on the basis of 8 oxygen

Si02	2.082	2.204	2.205	2.226	2.402	2.215	2.164	2.569
Al203	1.782	1.788	1.785	1.761	1.605	1.781	1.828	1.619
Fe0	0.247	0.022	0.022	0.023	0.032	0.017	0.020	0.035
Ca0	0.860	0.811	0.811	0.800	0.585	0.810	0.846	0.641
Na0	0.109	0.152	0.157	0.160	0.339	0.140	0.127	0.311
K20	0.002	0.003	0.003	0.006	0.006	0.002	0.002	0.005
An	89.40	84.73	84.30	83.58	63.44	85.85	87.59	67.04
Ab	11.33	15.88	16.32	16.71	36.76	14.83	13.14	33.36
Or	00.20	00.31	00.31	00.62	00.65	00.22	00.20	00.52

note:The above data is based on several point analyses from E thinsections.